

Title	Energy Bands for Solid Xenon
Author(s)	Azuma, Masayoshi; Sato, Kei
Citation	物性研究 (1985), 43(6): 265-274
Issue Date	1985-03-20
URL	<a href="http://hdl.handle.net/2433/91535">http://hdl.handle.net/2433/91535</a>
Right	
Type	Departmental Bulletin Paper
Textversion	publisher

## Energy Bands for Solid Xenon

Masayoshi Azuma and Kei Sato  
Department of Physics, Faculty of Science,  
Niigata University, Niigata

(1984年12月21日受理)

MS method by Pendry and Capart was considered in the relativistic case and modified formulae of relativistic APW were obtained for the energy band calculation. On the basis of group theory, they were transformed to a symmetrized form and reduced to be suitable for the calculation. Energy bands for solid xenon were calculated nonrelativistically by MS method and relativistically by these formulae mentioned above. Relativistic effects were investigated.

### §1. Introduction

Recently, review articles<sup>1)</sup> appeared on the properties of rare gas solids. For solid xenon, energy band structure was calculated by Rössler<sup>2)</sup> with KKR method. In order to reproduce the experimental value for the band gap, however, he increased the muffintin potential constant in the interstitial region by about +0.5 Ry. In the recent nonrelativistic calculation by Baroni et al.<sup>3)</sup> with GOPW (Gaussian orthogonalized plane wave) method, there remain discrepancies from experimental values. Meanwhile, APW method described by Loucks et al.<sup>4,5)</sup> was improved by Pendry and Capart<sup>6)</sup> and proposed as MS (Modified Slater) method. Previously, we derived MS method by a variational calculation and examined it.<sup>7)</sup> In this work, we investigate relativistic effects. In the next section, applying our previous method used in our derivation of MS formulae, we obtain modified formulae of relativistic APW for the energy band calculation. In §3, by means of these formulae, energy bands are calculated for solid xenon, and discussed in the last section. In the early calculation by Reilly,<sup>8)</sup> relativistic effects were evaluated by first order perturbation theory with the orthogonalized plane wave method.

### §2. Formulations

In the nonrelativistic case, Pendry and Capart<sup>6)</sup> introduced MS method, by means of the pseudo-potential

$$\Gamma^{\text{MS}} = \sum_{\ell=\ell^*} \sum_{m=m^*} Y_{\ell m}(\theta, \phi) Y_{\ell m}^*(\theta', \phi') \left[ \frac{\delta(r-R)\delta(r'-R)}{R^2} \{L_{\ell}(E, R) - L_{\ell}^0(-V'^2, R_-)\} + P(r, R_-)\delta(r-r')(V'^2+E) \right]. \quad (1)$$

Where,

$$L_{\ell}(E, R) = \frac{\partial R_{\ell}(E, R)/\partial R}{R_{\ell}(E, R)},$$

$$P(r, R_-) = 1 \text{ for } r \leq R, \\ = 0 \text{ for } r > R,$$

$L_{\ell}^0(-V'^2, R_-)$ : operating on  $j_{\ell}(k_n r')$  yields

$$L_{\ell}^0(-V'^2, R_-)j_{\ell}(k_n r') = \left. \frac{\partial j_{\ell}(k_n r') / \partial r'}{j_{\ell}(k_n r')} \right|_{r'=R},$$

$R$ : a radius of the muffintin sphere.

Summation over  $\ell$  and  $m$  extends only over the relevant component  $\ell^*$  and  $m^*$ .

Though scattering effects decrease rapidly with angular momentum  $\ell$ , APW formulae for the energy band calculation demand an infinite summation over all values of  $\ell$ . Truncation at some  $\ell=L$  imposes unphysical restriction on the radial wave functions with  $\ell$  greater than  $L$ , and leads to poor convergence.<sup>9)</sup> In our previous investigation,<sup>7)</sup> formulae of MS method were derived by means of the variational approach. There was shown the improved onvergence property of MS method with respect to the angular momentum  $L$ . In order to take into account this effect in the relativistic case, we expand the wave function in the form shown in Eq. (2) similar to the one used in our previous work.<sup>7)</sup>

In the muffintin sphere,

$$\psi_i(r) = \sum_{(|\kappa| < L)} \sum_{\nu} A_{\kappa\nu} \begin{bmatrix} g_{\kappa}(r)\chi_{\kappa}^{\nu} \\ if_{\kappa}(r)\chi_{-\kappa}^{-\nu} \end{bmatrix} \\ + \sum_{(|\kappa| > L)} \sum_{\nu} \sum_{i} \sum_{m} \nu^m(\mathbf{k}_i) \left\{ \frac{\mu + |E_i|}{2|E_i|} \right\}^{1/2} 4\pi i^{\ell} C_{\ell 1/2}(J, \nu: \nu-m, m) Y_{\ell}^{\nu-m^*}(\hat{\mathbf{k}}_i) \\ \times \begin{bmatrix} j_{\ell}(k_i r) \chi_{\kappa}^{\nu} \\ \frac{i\hbar c \mathbf{k}_i \cdot \text{Sign}(\kappa)}{\mu + E_i} j_{\ell'}(k_i r) \chi_{-\kappa}^{\nu} \end{bmatrix} \quad (2)$$

in the interstitial region,

$$\psi_0(r) = \sum_i \sum_m v^m(k_i) \left\{ \frac{\mu + |E_i|}{2|E_i|} \right\}^{1/2} \left[ \begin{array}{c} \chi(m) \\ \frac{\hbar c \mathbf{k}_i \cdot \boldsymbol{\sigma}}{\mu + E_i} \chi(m) \end{array} \right] \exp[i\mathbf{k}_i r]$$

Where

$$\mu = mc^2,$$

$$E_i = (\mu^2 + \hbar^2 c^2 k_i^2)^{1/2},$$

$C_{\nu}^{j, m}$  ( $J, \nu: \nu - m, m$ ): Clebsch-Gordan coefficients,

$\boldsymbol{\sigma}$ : the Pauli spin matrices,

$\chi(m)$ : the Pauli spinor,

$\chi_k^\nu$ 's: spin-angular orbitals.

A functional to be used in the relativistic case<sup>10</sup> is shown in Eq. (3).

$$I = \int d\tau \psi^\dagger \{ c\boldsymbol{\alpha} \cdot \mathbf{p} + \mu\beta + V(r) - E \} \psi - i \frac{\hbar c}{2} \int_{r=a} dS (\psi_i^\dagger + \psi_0^\dagger) \boldsymbol{\alpha} \cdot \mathbf{n} (\psi_0 - \psi_i). \quad (3)$$

Where  $\boldsymbol{\alpha}$  and  $\beta$  are  $4 \times 4$  matrices in the Dirac equation for an electron. Hereafter, we denote the radius of the muffintin sphere by  $a$ , and the surface integral in eq. (3) extends over the surface of the muffintin sphere. The expansion coefficients  $A_{\kappa\nu}$  are chosen such that the upper components of  $\psi_i$  and  $\psi_0$  are equal on the muffintin sphere.<sup>10</sup> Inserting the expression in Eq. (2) for the wave function into Eq. (3), after elimination of scattering effects for those components with  $\kappa$  in which  $|\kappa|$  is greater than  $L$ , we obtain the following modified secular equation of relativistic APW by variational calculation similarly as in Ref. 7.

$$\sum_{j, m'} v^{m'}(k_j) \left[ (E_i - E) \cdot \Omega \cdot \delta_{m, m'} \cdot \delta_{\mathbf{k}_i, \mathbf{k}_j} - 4\pi (E_j - E) \left\{ \frac{\mu + |E_i|}{2|E_i|} \right\}^{1/2} \left\{ \frac{\mu + |E_j|}{2|E_j|} \right\}^{1/2} \right. \\ \left. \times (\delta_{mm'} \left\{ 1 + \frac{\hbar^2 c^2}{(\mu + E_i)(\mu + E_j)} (\mathbf{k}_i \cdot \mathbf{k}_j \pm i [\mathbf{k}_i \times \mathbf{k}_j] \cdot \mathbf{e}_z) \right\} \right. \\ \left. + i \frac{\hbar^2 c^2}{(\mu + E_i)(\mu + E_j)} [\mathbf{k}_i \times \mathbf{k}_j] \cdot (\mathbf{e}_x \mp i \mathbf{e}_y) (1 - \delta_{mm'}) \right)$$

$$\begin{aligned}
 & \times \sum_{\ell=0}^L (2\ell+1) P_{\ell}(\hat{k}_i \cdot \hat{k}_j) F_{\ell}(k_i, k_j, a) \\
 & + (4\pi)^2 \hbar c a^2 \left\{ \frac{\mu + |E_i|}{2|E_i|} \right\}^{\frac{1}{2}} \left\{ \frac{\mu + |E_j|}{2|E_j|} \right\}^{\frac{1}{2}} \sum_{\kappa=-L}^L \sum_{\nu} C_{\ell \frac{1}{2}}(j, \nu: \nu-m, m) \\
 & \times C_{\ell \frac{1}{2}}(J, \nu: \nu-m', m') Y_{\ell}^{\nu-m}(\hat{k}_i) Y_{\ell}^{\nu-m'}(\hat{k}_j) j_{\ell}(k_i a) \\
 & \times \left\{ \frac{j_{\ell}(k_j a) f_{\kappa}(a)}{g_{\kappa}(a)} - \frac{\hbar c k_j \cdot \text{Sign}(\kappa)}{\mu + E_j} j'_{\ell}(k_j a) \right\} \\
 & + (4\pi)^2 (E_j - E) \left\{ \frac{\mu + |E_i|}{2|E_i|} \right\}^{\frac{1}{2}} \left\{ \frac{\mu + |E_j|}{2|E_j|} \right\}^{\frac{1}{2}} \sum_{\nu} \left\{ C_{L \frac{1}{2}}(L + \frac{1}{2}, \nu: \nu-m, m) \right. \\
 & \times C_{L, \frac{1}{2}}(L + \frac{1}{2}, \nu: \nu-m', m') Y_L^{\nu-m}(\hat{k}_i) Y_L^{\nu-m'}(\hat{k}_j) \\
 & \left. + C_{L+1, \frac{1}{2}}(L + \frac{1}{2}, \nu: \nu-m, m) C_{L+1, \frac{1}{2}}(L + \frac{1}{2}, \nu: \nu-m', m') \right. \\
 & \left. \times Y_{L+1}^{\nu-m}(\hat{k}_i) Y_{L+1}^{\nu-m'}(\hat{k}_j) \frac{\hbar c k_i}{\mu + E_i} \frac{\hbar c k_j}{\mu + E_j} \right\} F_L(k_i, k_j, a) = 0. \tag{4}
 \end{aligned}$$

Where,

$\Omega$  : the volume of the unit cell,

$$F_{\ell}(k_i, k_j, a) = \begin{cases} \frac{a^2}{k_i^2 - k_j^2} \{ j_{\ell}(k_i a) j'_{\ell}(k_j a) - j'_{\ell}(k_i a) j_{\ell}(k_j a) \} & \text{for } k_i \neq k_j, \\ \frac{a^3}{2} \left\{ \left[ 1 - \frac{\ell(\ell+1)}{k_i^2 a^2} \right] j_{\ell}^2(k_i a) + \frac{j_{\ell}(k_i a) j'_{\ell}(k_i a)}{k_i^2 a} \right. \\ \left. + \frac{j_{\ell}'^2(k_i a)}{k_i^2} \right\} & \text{for } k_i = k_j \end{cases} \tag{5}$$

$\kappa$ ,  $\ell$ ,  $\ell'$  and  $J$  are related each other in the following way,

$\kappa > 0$	$\kappa = \ell$	$\ell' = \kappa - 1$	$J = \ell - \frac{1}{2}$
$\kappa < 0$	$\kappa = -\ell - 1$	$\ell' = -\kappa$	$J = \ell + \frac{1}{2}$

The quantities in the outermost brackets [ ] in Eq. (4) give the matrix element specified by  $(\mathbf{k}_i, m)$ -th row and  $(\mathbf{k}_j, m')$ -th column. The indices  $m$  and  $m'$  specify up (+) or down (-) spin state. Of the double sign, the upper one is for the case of  $m$ =up spin state and the lower one for  $m$ =down spin state.

For the convenience of calculation, putting  $\hbar=1$ ,  $m=\frac{1}{2}$  and  $e^2=2$ , we transform into a new system of units. In this system, the unit of length is the Bohr radius. The unit of energy is Ry. After incorporation of symmetry, our expression takes the final form.

$$\begin{aligned}
 & \sum_{j,m'} v^{m'}(\mathbf{k}_j) \sum_T D_{11}^\lambda(T)^* \left[ \left\{ \left( \frac{[c^2]}{2} \right) H(\mathbf{k}_i) - E \right\} \cdot \Omega \cdot u_{mm'}(T) \delta_{\mathbf{k}_i, \mathbf{k}_j} \right. \\
 & - 4\pi \left\{ \left( \frac{[c^2]}{2} \right) H(\mathbf{k}_j) - E \right\} \left\{ \frac{1+H(\mathbf{k}_i)}{2H(\mathbf{k}_i)} \right\}^{\frac{1}{2}} \left\{ \frac{1+H(\mathbf{k}_j)}{2H(\mathbf{k}_j)} \right\}^{\frac{1}{2}} \left( u_{mm'}(T) \right. \\
 & \times \left\{ 1 + \frac{1}{1+H(\mathbf{k}_i)} \cdot \frac{1}{1+H(\mathbf{k}_j)} (4/[c^2]) (\mathbf{k}_i \cdot \mathbf{k}'_j \pm i [\mathbf{k}_i \times \mathbf{k}'_j] \cdot \mathbf{e}_z) \right\} \\
 & \left. \left. + i u_{\bar{m}m'}(T) \frac{1}{1+H(\mathbf{k}_i)} \cdot \frac{1}{1+H(\mathbf{k}_j)} (4/[c^2]) [\mathbf{k}_i \times \mathbf{k}'_j] \cdot (\mathbf{e}_x \mp i \mathbf{e}_y) \right) \right. \\
 & \quad \times \sum_{\ell=0}^L (2\ell+1) P_\ell(\hat{\mathbf{k}}_i \cdot \hat{\mathbf{k}}'_j) F_\ell(\mathbf{k}_i, \mathbf{k}_j, a) \\
 & \left. + 4\pi a^2 \left\{ \frac{1+H(\mathbf{k}_i)}{2H(\mathbf{k}_i)} \right\}^{\frac{1}{2}} \left\{ \frac{1+H(\mathbf{k}_j)}{2H(\mathbf{k}_j)} \right\}^{\frac{1}{2}} \sum_{\kappa=-L}^L \sum_n u_{nm'}(T) B_\kappa^{ij'} \left[ \begin{matrix} n \\ m \end{matrix} \right] \cdot j_\ell(\mathbf{k}_i a) \right. \\
 & \quad \times \frac{[c] f_\kappa(a)}{g_\kappa(a)} j_\ell(\mathbf{k}_j a) - \frac{2\mathbf{k}_j \cdot \text{Sign}(\kappa)}{1+H(\mathbf{k}_j)} j_{\ell'}(\mathbf{k}_j a)
 \end{aligned}$$

$$\begin{aligned}
 & + 4\pi \left\{ \left( [c^2] / 2 \right) H(k_j) - E \right\} \left\{ \frac{1 + H(k_i)}{2H(k_i)} \right\}^{\frac{1}{2}} \left\{ \frac{1 + H(k_j)}{2H(k_j)} \right\}^{\frac{1}{2}} \\
 & \times \sum_n u_{nm'}(T) \left\{ B_{-(L+1)}^{ij'} \left[ \begin{matrix} n \\ m \end{matrix} \right] + B_{(L+1)}^{ij'} \left[ \begin{matrix} n \\ m \end{matrix} \right] \cdot (4 / [c^2]) \frac{k_i}{1 + H(k_i)} \right. \\
 & \left. \times \frac{k_j}{1 + H(k_j)} \right\} F_L(k_i, k_j, a) = 0 \quad (6)
 \end{aligned}$$

Where,

$$[c] = 274.07204,$$

$$H(k_i) = \left\{ 1 + (2k_i / [c])^2 \right\}^{\frac{1}{2}},$$

$$B_{\kappa}^{ij} \left[ \begin{matrix} + \\ + \end{matrix} \right] = |\kappa| P_{\varrho}(\hat{k}_i \cdot \hat{k}_j) + i \text{Sign}(\kappa) [\hat{k}_i \times \hat{k}_j] \cdot \mathbf{e}_z \cdot P'_{\varrho}(\hat{k}_i \cdot \hat{k}_j),$$

$$B_{\kappa}^{ij} \left[ \begin{matrix} - \\ + \end{matrix} \right] = i \text{Sign}(\kappa) P'_{\varrho}(\hat{k}_i \cdot \hat{k}_j) [\hat{k}_i \times \hat{k}_j] \cdot (\mathbf{e}_x - i\mathbf{e}_y),$$

$$B_{\kappa}^{ij} \left[ \begin{matrix} - \\ - \end{matrix} \right] = B_{\kappa}^{ij} \left[ \begin{matrix} + \\ + \end{matrix} \right]^*,$$

$$B_{\kappa}^{ij} \left[ \begin{matrix} + \\ - \end{matrix} \right] = -B_{\kappa}^{ij} \left[ \begin{matrix} - \\ + \end{matrix} \right]^*,$$

$T$ : the operation of the double group,

$D^{\lambda}_{11}(T)$ : the element of the representation matrix for the  $\lambda$ -representation of the double group,

$u_{mm'}(T)$ : the transformation matrix of the spinor in the double group,

$k_i$ : the progenitor wave vector.

$k'_j$  and  $j'$  show the wave vector transformed from  $k_j$  by the symmetry operation. In  $u_{\bar{m}m}(T)$ ,

$\bar{m}$  shows the other spin state than the one indicated by  $m$ . The sets of a wave vector and a spin state

$(k_i, m)$ 's are given by progenitors. Progenitors for  $\Gamma^+_6$  state are exhibited in Table I. NPRO indicates

the number of progenitors and corresponds to the dimension of the secular equation. NSPLW specifies

the dimension of the corresponding secular equation in the unsymmetrized case and is equal to

the number of spin plane wave states to be used.

Table I. Progenitors for  $\Gamma_6^+$  state. (Relativistic calculation).

NPRO	NSPLW	Progenitor ( $A/2\pi$ ) $k_i$		spin state	
1	2	(0,	0,	0)	-
2	18	(1,	1,	1)	-
3	30	(0,	2,	0)	-
4	54	(2,	2,	0)	-
5	102	(1,	3,	1)	-
6	102	(1,	3,	1)	+
7	118	(2,	2,	2)	-
8	130	(0,	4,	0)	-
9	178	(3,	3,	1)	-
10	178	(3,	3,	1)	+
11	226	(2,	4,	0)	-
12	226	(2,	4,	0)	+
13	274	(2,	4,	2)	-
14	274	(2,	4,	2)	+
15	290	(3,	3,	3)	-

(A: the lattice constant)

### §3. Energy Band Calculations

On account of the Ewald's method, the muffintin potential used in the previous self-consistent calculation of energy bands for solid argon<sup>11)</sup> has the following expression with the charge density  $\sigma(r)$ .

$$\begin{aligned}
 V(r) = & -\frac{2Z}{r} - \frac{2}{r} \int_0^r dr' 4\pi r'^2 \sigma(r') - 2 \int_r^a dr' 4\pi r' \sigma(r') \\
 & - 2\bar{\rho}_{\text{out}} \cdot \Omega \cdot \left[ \frac{4.58485}{a} - \frac{2\pi a^2}{\Omega} \right] + X\alpha(r)
 \end{aligned} \tag{7}$$

in the muffintin sphere,

$$= 2\bar{\rho}_{\text{out}} \cdot \Omega \cdot \left[ \frac{4.58485}{a} - \frac{3}{(R_W^3 - a^3)} \left\{ \frac{1}{2}(R_W^2 - a^2) - \frac{8\pi}{15a^3}(R_W^5 - a^5) \right\} \right]$$

+  $X\alpha(\bar{\rho}_{\text{out}})$  in the interstitial region.

Where,  $R_W$  is the radius of a sphere having the same volume as the Wigner-Seitz cell. Solid xenon has a lattice constant of 6.1317 Å.



In this work, overlapping the self-consistent nonrelativistic atomic charge densities placed at the lattice sites, we obtained the crystalline charge density  $\sigma(r)$ . Energy bands were calculated nonrelativistically and relativistically with the same potential evaluated by Eq. (7) from this crystalline charge density. Self-consistency was not pursued in this energy band calculation. As for the exchange potential, Hartree-Fock-Slater exchange, namely,  $X\alpha$ -potential with  $\alpha=1$  was assumed. Nonrelativistic energy bands were calculated by means of MS method and displayed in Fig. 1. The

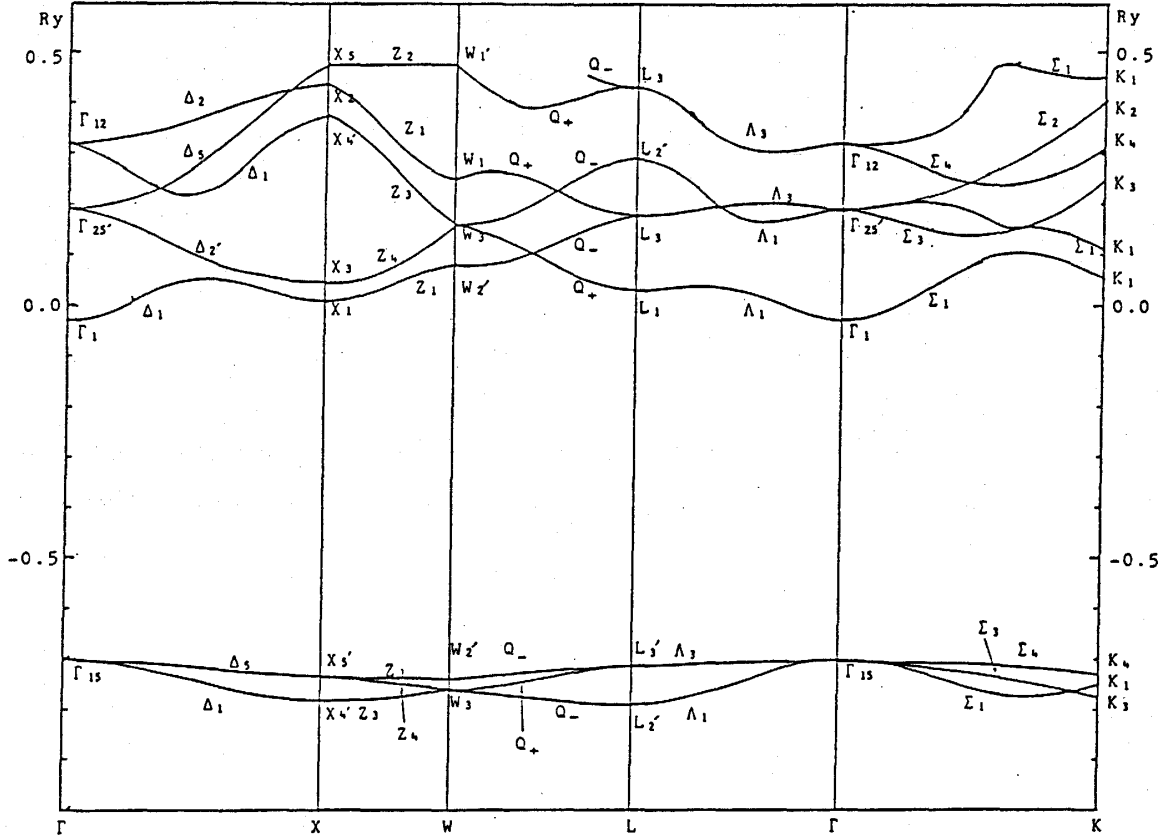


Fig. 1 Non-relativistic energy bands for solid Xe.

greatest difference from the energy bands for solid argon<sup>11)</sup> is the interchange of  $L'_2$  level and  $L_3$  level in the conduction bands. This displacement causes different behavior along symmetry lines  $\Lambda$  and  $Q$ . Relativistic energy bands were calculated by means of Eq. (6) described in the previous section and exhibited in Fig. 2. Especially, valence bands behave much differently from those non-relativistic results in Fig. 1. Surveying these two band structures, one nonrelativistic and the other relativistic, we can recognize the relationship between them. There can be seen the splittings of energy levels. These splittings just coincide with group theoretical predictions.<sup>12)</sup> Each pair of  $\Lambda_4$  and  $\Lambda_5$ ,  $Q_3$  and  $Q_4$ ,  $L^+_4$  and  $L^+_5$ , and  $L^-_4$  and  $L^-_5$  is degenerate owing to the time reversal symmetry. Gradually decreasing shifts of energy levels are found along with the increasing energy. In the semi-relativistic treatment by the Foldy-Wouthuysen transformation, these shifts are reduced to spin-

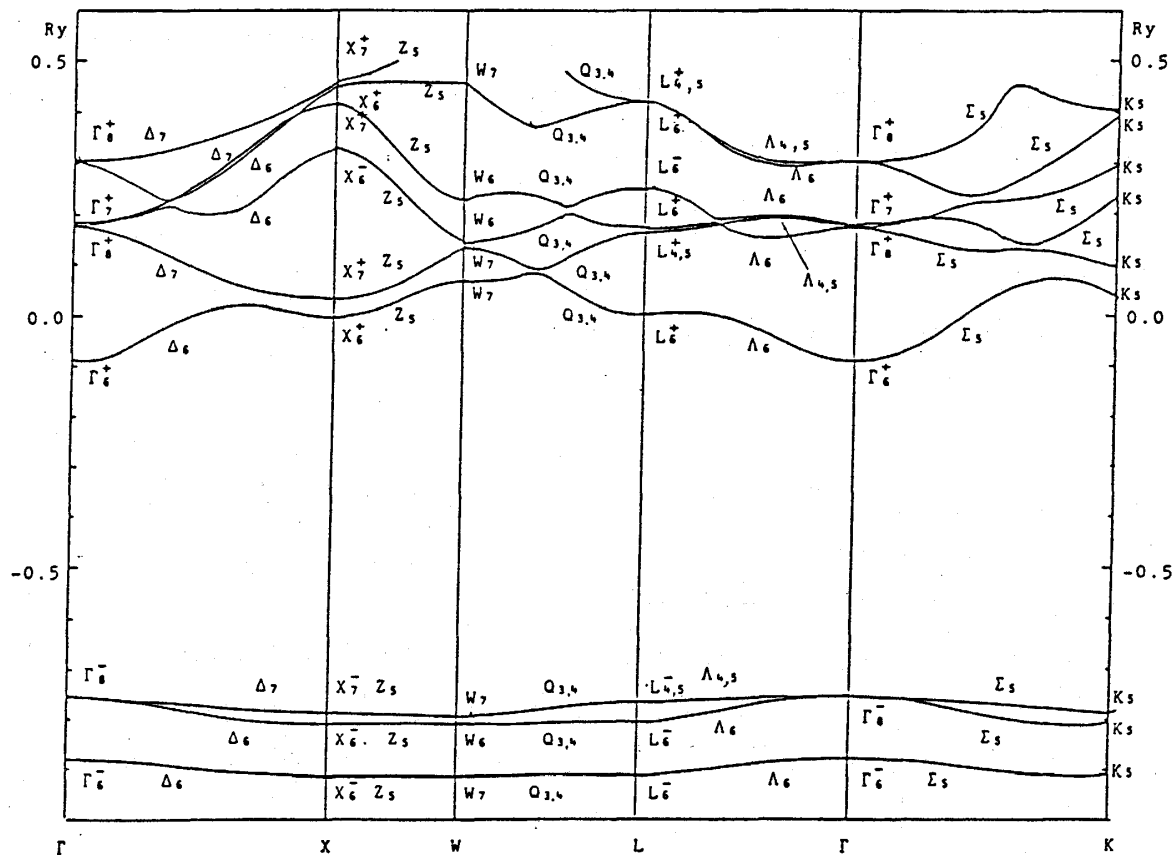


Fig. 2 Relativistic energy bands for solid Xe.

orbit splittings, mass-velocity corrections, and Darwin corrections.

#### §4. Discussion

These two results obtained nonrelativistically by MS on one hand, and relativistically by Eq. (6) on the other hand with the same potential, seem to confirm the reliability of these procedures. In order to resume the experimental band gap, Rössler<sup>2)</sup> increased the muffintin potential constant in the interstitial region by about +0.5 Ry. In our results, band gap to be compared with the experimental value<sup>13)</sup> of 9.3 eV is,  $E(\Gamma_1) - E(\Gamma_{15}) = 9.18$  eV in the nonrelativistic case and  $E(\Gamma_6^+) - E(\Gamma_8^-) = 9.15$  eV in the relativistic case. Baroni et al.<sup>3)</sup> obtained 13.78 eV nonrelativistically. In the experiment of photo-emission, the threshold energy for the excitation of a valence electron to the vacuum level positions the top of the valence band at -9.8 eV.<sup>14)</sup> Our nonrelativistic and relativistic top valence states lie at  $E(\Gamma_{15}) = -9.5$  eV and at  $E(\Gamma_8^-) = -10.27$  eV respectively. In Ref. 3, the valence band top was placed at  $E(\Gamma_{15}) = -11.11$  eV. From those experiments<sup>13, 14)</sup> of photo-absorption, photo-emission, and photo-conductivity, the bottom of the conduction bands is predicted to be at -0.5 eV. Our nonrelativistic and relativistic conduction band minima are at  $E(\Gamma_1) = -0.32$  eV and at  $E(\Gamma_6^+) = -1.22$  eV respectively. Baroni et al.<sup>3)</sup> placed it at  $E(\Gamma_1) = 2.67$  eV. Though further investigation is desirable, the overall behavior of the energy bands obtained above seems to be reason-

Masayoshi Azuma and Kei Sato

able. In this work, relativistic effects were investigated through the nonrelativistic calculation by MS and the relativistic calculation by Eq. (6) with the same potential. For these purposes, these symmetrized formulae were especially suitable.

### Acknowledgment

We calculated with facilities at Niigata University Information Center.

### References

- 1) M. L. Klein and J. A. Venables ed., *Rare Gas Solids* (Academic Press, London) Vol. 1 (1976), Vol. 2 (1977), Vol. 3 (1981).
- 2) U. Rössler, *Phys. Status Solidi* **42** (1970) 345.
- 3) S. Baroni, G. Grosso and G. Pastori, Parravicini, *Phys. Status Solidi (b)* **110** (1982) 227.
- 4) T. L. Loucks, *Augmented Plane Wave Method* (Benjamin, New York, 1967).
- 5) J. O. Dimmock, *Solid State Physics* (Academic Press, New York and London, 1971) Vol. 26, p. 103.
- 6) J. B. Pendry and G. Capart, *J. Phys.* **C2** (1969) 841.
- 7) M. Azuma, *J. Phys. Soc. Jpn.* **44** (1978) 339.
- 8) M. H. Reilly, *J. Phys. Chem. Solids* **28** (1967) 2067.
- 9) J. M. Ziman, *Solid State Physics* (Academic Press, New York and London, 1971) Vol. 26, p. 90.
- 10) T. L. Loucks, *Phys. Rev.* **139** (1965) A1333.
- 11) M. Azuma, *J. Phys. Soc. Jpn.* **49** (1980) 2141.
- 12) F. Bassani and G. Pastori Parravicini, *Electronic States and Optical Transitions in Solids* (Pergamon press, Oxford and New York, 1975).
- 13) U. Asaf and I. T. Steinberger, *Phys. Rev.* **B10** (1974) 4464.  
D. Pudewill, F. J. Himpsel, V. Sail, N. Schwentner, M. Skibowski and E. E. Koch, *Phys. Status Solidi (b)* **74** (1976) 485.
- 14) N. Schwentner, M. Skibowski and W. Steinmann, *Phys. Rev.* **B8** (1973) 2965.  
N. Schwentner, F. J. Himpsel, V. Sail, M. Skibowski, W. Steinmann and E. E. Koch, *Phys. Rev. Lett.* **34** (1975) 528.